PCCP

Accepted Manuscript

ROYAL SOCIETY OF CHEMISTRY

www.rsc.org/pccp

Physical Chemistry Chemical Physics RSCPublishing

ARTICLE

Novel Benzimidazole Salts for Lithium Ion Battery Electrolytes: Effects of Substituents

Cite this: DOI: 10.1039/x0xx00000x

T. Sriana, E. G. Leggesse*, and J. C. Jiang*

Received 00th xxxx 2015,
Accepted 00th xxxx 2015

DOI: 10.1039/x0xx00000x

www.rsc.org/

In this paper, we report on our effort to design a novel lithium salt derived from bis(trifluoroborane)benzimidazolide by using density functional theory (DFT) calculations. The effects of different substituents are investigated with respect to ion pair dissociation energies and intrinsic anion oxidation potential of the molecules. Based on our calculations, we have found that, ion pair dissociation energies and intrinsic anion oxidation potentials of the anions mainly affected by the position and type of substituents introduced on the parent structure. Compared to $-CH_3$, substitution at C2 position of the parent benzimidazole (B^-) moiety by $-CF_3$ results an increase in anion oxidation stability. However, we observed a negligible change in intrinsic anion oxidation potential as the length of the fluoroalkyl group increased to $-C_2F_5$. The most promising anions are generated by considering double-substitution at C2 and C5 positions. Among the possible anions, bis(trifluoroborane)-5-nitro-2-(trifluoromethyl) benzimidazolide ($BTNTB^-$), with the calculated intrinsic anion oxidation potential of 5.50 V vs. Li^+/Li, can be considered as a potential candidate for high voltage Li-ion battery.

1. Introduction

The Lithium-ion batteries (LIBs) have become the dominant power source for portable electronic devices cordless tools and laptops due to their intrinsic advantages such as high energy density, superior rate capability, high efficiency and long life cycle compared with other battery technologies.[1-3] Moreover, owing to the great advancement in the past decades this technology is also considered as promising source of energy for hybrid electric vehicles (HEVs), plug-in hybrid electrical vehicles (PHEVs) and stationary energy storage systems for solar and wind energy.[4, 5] However, there are several challenges that need to be addressed in the development of improved LIBs such as improvement of high-temperature performance and minimizing capacity fading during prolonged charge-discharge cycling.[4] A significant element that limits the performance and the safety of existing LIBs relates to the salt that is commonly used in these battery systems.

Ever since the commercialization of the rechargeable Li-ion cell, $LiPF_6$ is by far the most widely used electrolyte salt.[6] It produces electrolyte solutions with a superior ion conductivity, good electrochemical oxidation stability and adequate thermal stability when dissolved in binary or ternary solvent systems of cyclic carbonates.[7] Moreover, $LiPF_6$ based electrolyte systems prepared from cyclic and acyclic organic carbonates are reported to exhibit good protective surface film formation properties on the graphite anode and the aluminum current collector.[6] However, Regardless of the high conductivity of electrolytes with $LiPF_6$, they suffer from limited thermal and chemical stability. $LiPF_6$ can undergo an autocatalytic decomposition into LiF and PF_5 in which PF_5 will react irreversibly with a trace amount of water and carbonate solvents in the electrolyte which lead to safety hazards. In addition, its limited thermal stability makes the salt a poor choice when developing electrolytes for LIBs with wider working temperature range.[8-13]

In recent years, various researches on lithium salts have been reported and focused on the development of suitable anions which can coordinate with lithium cation and produces electrochemically and thermally stable salts.[10, 14-17] lithium fluoroalkyl phosphates (LiFAP) which is generated by substitution of fluorine atoms of $LiPF_6$ with electron withdrawing perfluorinated alkyl groups is reported to be superior to $LiPF_6$ as an electrolyte for both graphite anodes and $LiMn_2O_4$ cathodes.[18, 19] The observed improved performance was attributed to the stabilization of P-F bonds owing to the steric shielding of the phosphorus by the hydrophobic perfluorinated alkyl groups as well as the formation of fluorinated surface species which leads to the stabilization of the electrodes.[19, 20] New classes of lithium salts based on boron containing anions, which exhibits chelating properties have been reported.[21-25] LiBOB, which was first reported by Xu and Angell,[16] is one of the most promising of these new salts. Even though, it has high thermal stability, the low solubility, higher viscosity and lower conductivity of its electrolytes significantly influences the performance of the battery. Other borate salts, such as lithium difloro[oxalato]borate (LiDFOB)[26] and lithium (malonato oxalato) borate (LiMOB)[27] were also synthesized and reported to have an improved properties as compared to LiBOB such as lower interfacial resistance and better power capability.

An alternative approach to design new lithium ion battery salts have been also explored by considering designing substituted heterocyclic anions.[28, 29] Barbarich et al. report a new

class of lithium salt based on imidazole and concluded that the anion in lithium bis(trifluoroborane)imidazolide show a high degree of charge delocalization making the salt more conductive and stable compared to $LiPF_6$.[29] Similarly, new potential anions were proposed by extending the imidazole ring to benzimidazole ($C_7H_6N_2$).[30] In 2010, Scheers et al.[31] also reported 4,5,6,7-tetracyano-2-trifluoromethyl benzimidazolides (TTB) and 4,5,6,7-tetracyano-2-pentafluoromethyl benzimidazolides (PTB) for high voltage Li-ion battery application. Chern et al.[32] recently reported new cyano-substituted bis(trifluoroborane)benzimidazolide salts as a replacement for the commonly used $LiPF_6$. They have found that the new cyano-substituted derivatives of bis(trifluoroborane)benzimidazolide showed excellent thermal stability, high conductivity and better electrochemical stability. Moreover, the reported salts were soluble in commonly used cyclic or acyclic alkyl carbonate solvents.

In this work, we will employ bis(trifluoroborane)-benzimidazole as parent structure and identify potential anion candidates by using density functional theory (DFT) calculations. New anion structures were proposed by considering mono-substitution on the imidazole hydrogen with $-CH_3$, $-CF_3$ or $-C_2F_5$ and then by substitution on the benzene ring with electron withdrawing groups (-F, -CHO, -CN, $-SO_2CH_3$ and $-NO_2$). The effect of different substituent will be investigated with respect to ion pair dissociation energy and anion oxidative stability of the molecule.

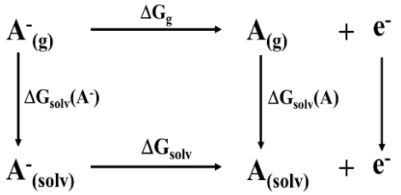

Fig. 1 Thermodynamic cycle proposed for the oxidation reaction of the anions ($A^- \rightarrow A + e^-$).

2. Computational Details

All geometry optimizations and frequency determinations are performed using the Gaussian 09 package.[33] Density functional theory (DFT) has been selected with B3LYP method, which is hybrid functional, containing Becke's three-parameter exact exchange function (B3) in conjunction with nonlocal gradient-corrected correlation function of Lee-Yang-Parr (LYP).[34-37] B3LYP has been applied with triple split valence basis set 6-311G along with a set of p, d polarization function on heavy atoms and hydrogen atoms.[38, 39] Spin-unrestricted calculations are used to allow for any possible bond cleavage during geometry optimization of the radical species.[40]

The relative energies with ZPE correction, Gibbs free energies, and enthalpies are calculated at 298.15 K. Basis set superposition errors (BSSEs) were checked for the ion pair configurations and anions by employing Boys-Berrnardi counterpoise correction.[41] The calculated BSSEs were found to be <5 kcal mol^{-1} thus are excluded as they will not cause any significant changes in the calculations of dissociation energies. The natural bond orbital (NBO) method was used to calculate the natural population analysis (NPA) charges and second-order perturbation energies using NBO program include in the Gaussian program package.[42] For all calculated system, the solvent effect is addressed by employing the universal model proposed by Marenich et al. based on Density (SMD).[43] In this universal solvation model, which is the recommended method for calculating solvation free energies, the solute electron density is employed regardless of the partial atomic charges.[43, 44] A dielectric constant of 46.35, an average value between the dielectric constant of EC (89.6) and DMC (3.1) is adopted to implicitly account for solvent effects in EC/DMC (1:1) solvent system.

Eleven anion structures were generated by considering different substitution on the benzene and imidazole moieties of bis(trifluoroborane)benzimidazolide (BTB^-) as shown in Fig. 2. The structures for the generated anions are shown in Fig. S1 of the Supporting Information. New anion structures were proposed by considering mono-substitution at C2 (hereafter referred to as R1) position with $-CH_3$, $-CF_3$ or $-C_2F_5$ and then by substitution at the C5 (hereafter referred to as R2) position with electron withdrawing groups (-F, -CHO, -CN, $-SO_2CH_3$ and $-NO_2$). Symmetric anion structures can be found via mono-substitution ($-CH_3$, $-CF_3$ or $-C_2F_5$) at R1 position to form bis(trifluoroborane)-2-methylbenzimidazolide(BTMB), bis(trifluoroborane)-2-(trifluoromethyl)benzimidazolide(BTTB) and bis(trifluoroborane)-2-(pentafluoroethyl)benzimidazolide (BTPB) respectively.

Similarly, asymmetric anion structures can be generated when electron withdrawing groups (-F, -CHO, -CN, $-SO_2CH_3$, and $-NO_2$) are substituted on R2 position to form bis(trifluoroborane)-5-fluorobenzimidazolide (BTFB), bis(trifluoroborane)-5-carbaldehydebenzimidazolide (BTAB), bis(trifluoroborane)-5-cyanobenzimidazolide (BTCB), bis(trifluoroborane)-5-methanesulfonylbenzimidazolide (BTSB), and bis(trifluoroborane)-5-nitrobenzimidazolide (BTNB), respectively. Double-substitution at R1 and R2 positions with $–CF_3$ and $–NO_2$, respectively, will also result in the generation of asymmetric anion structure namely bis(trifluoroborane)-5-nitro-2-(trifluoromethyl) benzimidazolide (BTNTB).

In order to find the most stable lithium ion pair configurations, more than ten starting structures were generated for each anions, by randomly positioning the lithium cation at mono-, bi-, and tridentate coordination sites, around $–BF_3$, the imidazole moiety and the substituents. Each geometry was then optimized using DFT in order to find the energy minimum configuration from respective sets.

To estimate the dissociation of the ion pairs, dissociation energy (ΔE_d) is calculated for lithium salt by using Equation 1. Based on the equation, the smaller the energy difference, the more dissociative the corresponding salt.

$$\Delta E_d = \{E[Li^+] + E[anion^-]\} - E[salt] \quad (1)$$

A thermodynamic cycle (Fig. 1) is used to calculate the Gibbs free energy change to determine the electrochemical intrinsic anion oxidation potentials of the anions. The solvation free energy of the neutral molecule (A), the anion (A^-) and gas phase redox energies are denoted by $\Delta G_{solv}(A)$, $\Delta G_{solv}(A^-)$ and ΔG_g respectively. The Gibbs free energy change for the oxidation reaction can be calculated as shown in Eq. 2.

$$\Delta G_{solv} = \Delta G_g + \Delta G_{solv}(A) - \Delta G_{solv}(A^-) \quad (2)$$

Table 1. Optimized geometries of free anions and ion pairs calculated with B3LYP/6-311++G(d, p), values are given in Å

Structures	Anion				Lithium ion pair				
	N3-C2	N4-C2	N3-B	N4-B	N3-C2	N4-C2	N3-B	N4-B	Li-F
B	1.347	1.347	-	-	1.374	1.318	-	-	-
BTB	1.335	1.335	1.567	1.567	1.356	1.318	1.504	1.628	1.809
BTMB	1.346	1.346	1.575	1.575	1.365	1.328	1.512	1.632	1.822
BTTB	1.343	1.343	1.605	1.605	1.364	1.324	1.534	1.690	1.827
BTPB	1.344	1.344	1.602	1.602	1.366	1.325	1.532	1.681	1.828
BTFB	1.337	1.337	1.568	1.568	1.359	1.315	1.505	1.631	1.813
BTAB	1.338	1.332	1.572	1.572	1.352	1.320	1.513	1.635	1.820
BTCB	1.333	1.337	1.573	1.573	1.355	1.318	1.510	1.637	1.821
BTSB	1.334	1.337	1.574	1.573	1.353	1.321	1.519	1.636	1.845
BTNB	1.332	1.340	1.576	1.577	1.353	1.320	1.514	1.639	1.823
BTNTB	1.339	1.346	1.617	1.615	1.361	1.326	1.542	1.707	1.835

The Nernst equation has been used to calculate one-electron thermodynamic oxidation potential (E_{ox}) versus Li^+/Li as shown in Eq. 3.

$$E_{ox}(Li^+/Li) = -\left[\frac{\Delta G_{solv}}{F}\right] - 1.46V \quad (3)$$

where F is Faraday constant and 1.46 V is used to convert the absolute electrochemical potential to experimentally measured Li^+/Li potential scale.[45]

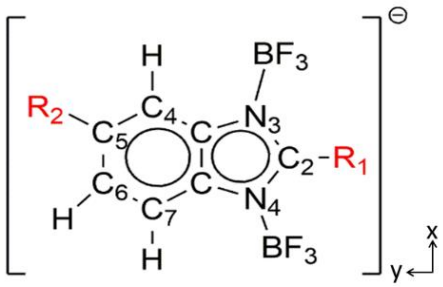

$\mathbf{R_1}$ = H, CH_3, CF_3, C_2F_5
$\mathbf{R_2}$ = H, F, CHO, CN, SO_2CH_3, NO_2

Fig.2 Structure of the parent molecule with two substitution sites designated as R1 and R2.

3. Results and Discussion

3.1. Geometries of the anions

Table 1 lists some of the geometrical features of the most stable anions and ion pair structures. From the Table, it can be seen that, the bond lengths of N3-C2 and N4-C2 increased as a result of substitution at the R1-position. This fact can be attributed to the inductive effect of the substituents which increase the electron density on the imidazole ring. The greater negative inductive effect of the substituent (-F, -CHO, -CN, $-CH_3SO_2$, and $-NO_2$) at the R2-position results in slight shortening of the N3-C2 and N4-C2 bonds compared with BTB^-. On the other hand, substitution either at the R1 or R2 positions increases the N3-B and N4-B bond lengths due to the steric repulsion. The greater elongation of the N3-B and N4-B bonds for $BTTB^-$ and $BTPB^-$ can be attributed to the stronger steric interaction of the trifluoroborate with trifluoromethyl and the relatively bulky pentafluoroethy substituents. Similarly, compared to the molecules generated via mono-substitution, slightly longer N3-C2, N4-C2 and N3-B bond lengths were observed for $BTNTB^-$. It is interesting to note that average interatomic distance between the fluorine atoms of trifluoroborate and the substituents at R1 ($-CF_3$ or $-C_2F_5$) can be used as a rough indicator of the observed steric hindrance. The average distances between adjacent fluorine atoms in $BTTB^-$ and $BTPB^-$ were found to 2.921 and 2.855 Å, respectively. Since the van der Waal radius of fluorine atom is about 1.470 Å, the calculated interatomic distances are enough to predict the existence of steric effect.[46] Previous studies also showed that, trifluoromethyl has steric effect which is comparable to the relatively bulky isopropyl group.[47, 48]

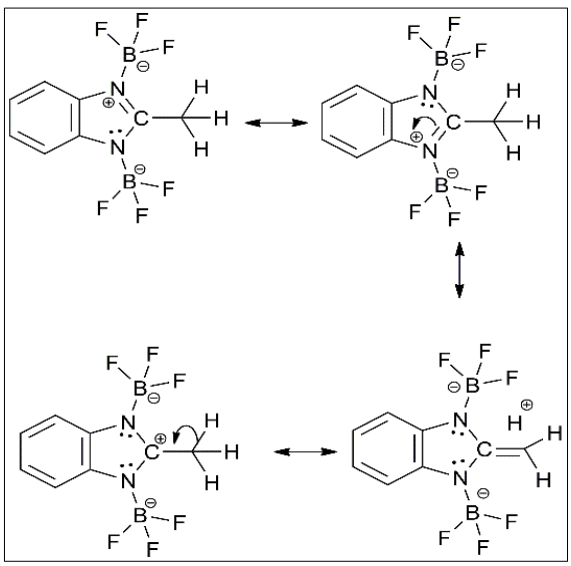

Fig.3 The influence of hyperconjugation in methyl substituted BTB^-. Here one of the carbon-hydrogen bonds of CH3 lie in the plane of π-bond orbital resulting in the delocalization of π-electrons without the apparent release of the hydrogen.

3.2. Lithium ion pair configurations

For all derivatives of bis(trifluoroborane)-benzimidazole, we have found that the most stable configurations are coordinated with two fluorine to form the bidentate ion pairs. A monodentate ion pair configuration was also found to be the most stable structure for B^-, in which the N3-C2 elongates by 0.026 Å. Compared with the reported equilibrium Li-F distance in $LiBF_4$ (1.583 Å),[49] the Li-F distance in LiBTB is elongated by 0.226 Å, showing a weaker interaction between the cation and the anion . The average equilibrium Li-F distance in LiBTNTB is relatively longer than the corresponding distances in other lithium ion pairs. This indicates that LiBTNTB, which is formed via double-substitution at the R1 and R2 positions, is easier to dissociate compared to those with mono-substitution on the benzimidazole structure.

For the detail analysis of the substituent effect on the parent structure, the sum of natural charges of the ring and the substituent moieties were calculated for the anions and the corresponding lithium ion pair configurations, as listed in Table 2. As can be seen from the table, the natural charge of the ring in BTB^- becomes less negative compared to that of B^- as a result of the electron-withdrawing nature of the Lewis acid, BF_3. A close examination of the ion pairs also reveals that, the positive charge on Li^+ increases in all substituted systems, with the highest value obtained from the doubly substituted configuration, LiBTNTB. The increase in the positive charge can be ascribed to a decrease in the electron transfer from the anion to cation. The charge on the ring moiety became less negative in the substituted derivatives compared to the parent structure due to the electron withdrawing effect of the substituents.

Table 2. Atomic charges of the free anions and lithium ion pairs calculated with B3LYP/6-311++G(d, p), values are given in natural charge

Structures	Anion				Lithium ion pair				
	ΣQ_{ring}	BF_3 (1)	BF_3 (2)	Substituent	ΣQ_{ring}	BF_3 (1)	BF_3 (2)	Substituent	Li
B	-2.017	-	-	-	-1.895	-	-	-	0.956
BTB	-1.378	-0.398	-0.398	-	-1.296	-0.442	-0.327	-	0.972
BTMB	-1.226	-0.397	-0.397	0.094	-1.177	-0.439	-0.333	0.094	0.974
BTTB	-1.222	-0.374	-0.374	0.028	-1.203	-0.424	-0.295	0.058	0.973
BTPB	-1.204	-0.374	-0.374	0.011	-1.175	-0.425	-0.298	0.038	0.973
BTFB	-0.833	-0.395	-0.395	-0.373	-0.781	-0.440	-0.325	-0.355	0.973
BTAB	-1.013	-0.368	-0.368	-0.030	-1.124	-0.429	-0.321	-0.010	0.973
BTCB	-1.155	-0.390	-0.390	-0.062	-1.124	-0.434	-0.318	-0.027	0.973
BTSB	-1.310	-0.390	-0.390	0.076	-1.031	-0.424	-0.319	0.119	0.972
BTNB	-0.908	-0.387	-0.387	-0.350	-0.921	-0.429	-0.316	-0.281	0.973
BTNTB	-0.769	-0.363	-0.363	-0.336 ($-NO_2$), 0.040 ($-CF_3$)	-0.837	-0.414	-0.281	-0.204	-0.272 ($-NO_2$), 0.068 ($-CF_3$)

It is known that when CH_3 is attached to a saturated or unsaturated carbon it will increase the electron density on the adjacent group since it acts as an indicative electron donating group. However, in $BTMB^-$, the charge on the ring moiety became less negative compared to BTB^- due to the hyperconjugation effect as shown in the Fig. 3. This effect arises due to the partial overlap of a sp3-s (C-H bond) with the empty π-orbital of the positively charged carbon atom (C2).[50] Moreover, the electron delocalization is favored by the planarity of the molecule which allows maximum overlap between the adjacent atomic orbitals. As illustrated in Table 3, the results of dipole moment showed only one component in the y direction indicative of the planarity of the molecules. Hence, one of the C-H bond of CH_3 can align in plane of the empty π-orbital allowing the delocalization of the electrons of C-H bond into the empty π-orbitals. The displacement of the electron pair of the C-H bond in CH_3 causes a partial positive charge on the hydrogen atom without the actual proton release. This type of overlap stabilizes the lithium cation as the electron density from the sigma bond helps in dispersing the positive charge.

Fig. 4 shows the HOMO and LUMO plot of the parent molecule obtained from NBO analysis. As can be seen from the Fig., substantial HOMO and LUMO coefficient were found on C5 while only the LUMO coefficient was found on C2. Hence, it can be expected that substitution on R1 will have a significant effect on the LUMO whereas both the LUMO and HOMO will be affected by substitution on R2. As presented in Table 3, introducing electron-withdrawing group on R1 results a decrease in the energy level of the HOMO and the LUMO, with a significant change noted on the LUMO. Similarly, introducing CH_3, which is electron donating group by inductive effect, results in an increase in the HOMO and the LUMO energies. Substitution on R2 by electron withdrawing group also decreases the energy level of the HOMO and LUMO. Amongst the possible substituents, fluorine is the only one whose electron withdrawing inductive effect is strong enough to compensate the electron donating effect, which allows for a possible interplay with the parent structure.

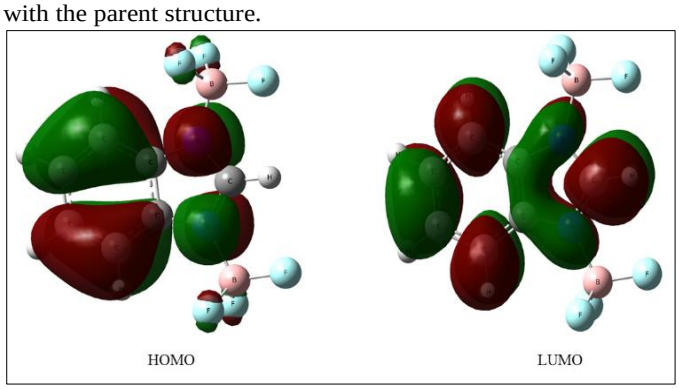

Fig.4 The LUMO and HOMO of BTB anion in a solvent phase at an isovalue = 0.02 in atomic units.

Table 3. The HOMO and LUMO energy levels (ev) and y-component dipole moments in Debye (μ_y) of the parent structure and its derivatives

Structure	R1	R2	HOMO	LUMO	μ_y
BTB	H	H	-6.80	-1.16	7.32
BTMB	CH_3	H	-6.66	-1.02	5.49
BTTB	CF_3	H	-6.89	-1.78	7.21
BTPB	C_2F_5	H	-6.89	-1.78	4.83
BTFB	H	F	-6.75	-1.27	6.53
BTAB	H	COH	-6.99	-2.24	7.64
BTCB	H	CN	-7.07	-1.76	4.17
BTSB	H	SO_2CH_3	-7.13	-1.62	10.14
BTNB	H	NO_2	-7.21	-3.08	4.53
BTNTB	CF_3	NO_2	-7.34	-3.13	2.50

As can be seen from Table 3, the negative inductive effect of fluorine leads to stabilization of the HOMO and LUMO orbitals. However, the resonance effect leads to a destabilization of the HOMO orbital relative to the LUMO orbital due to the low-lying p_z orbitals of fluorine with respect to the HOMO orbital of conjugated system. Hence, the HOMO energy of $BTFB^-$ increases compared to BTB^-. Fluorine, which is a weaker electron withdrawing group, exerts strong field and inductive effects on the C5 atom. Additional electron density cannot be withdrawn by resonance since there are no available vacant orbitals. However, the lone-pair electrons on the fluorine can be donated by resonance. As a result of this push-pull effect, the resonance and the positive inductive effects of the substituted fluorine nearly canceled out. Previous researches have shown that lithium salt dissociation plays a great role in determining the conductivity of the electrolyte solution, thereby affecting the overall battery's performance.[51-53] It is known that the conductivity or mobility of a particular salt is determined by factors such as the size of the ions, the number of ions and the charge on the ions in the solution. Studies indicated that, the conductivity of various salts in non-aqueous electrolytes in lithium ion batteries the number of freely available ions plays a crucial role in determining the electric conductivity of the battery.[51, 52]

Table S1 of the Supporting Information shows the calculated dissociation energies for the ion pair configurations in both gas and solvent phase. The BSSEs corrected and BSSEs-free dissociation energies are shown in the Table for the sake of comparison. It is interesting to note that the BSSEs corrections do not alter the order of the values of the dissociation energies. Considering implicit solvation models lead to further decrease in the dissociation energies as a result of stabilization of the species by the dielectric response. However, for each ion pair configuration, the vacuum and solvent calculations give the same qualitative results and trends. Compared to LiB, LiBTB exhibits a weaker coordination because of relatively extensive charge delocalization. In the benzimidazole anion, a single negative charge is distributed across the anion which is then stabilized by the positive core. However, introducing electron-withdrawing group, BF_3, results in the formation of BTB anion which shows extensive charge delocalization.[54] When compared to previously reported gas-phase dissociation energies of commonly used lithium salts, it can be seen that, all the salts presented in this study can easily dissociate. (131, 135, 140 and 116 kcal mol^{-1} for $LiPF_6$, $LiClO_4$, LiTFSI, and LiBOB, respectively).[55, 56]

Natural bond orbital analysis can also be used further to analyze the charge transfer and stability of the ion pair configuration. The donor (anion)-acceptor (Li^+) interactions can safely be treated by the second-order perturbation energy ($E_{(2)}$) given in the NBO theory as: ($E_{(2)} = \Delta E_{ij} = q_i (F_{ij})^2/\Delta\varepsilon$) where q_i is the donor orbital occupancy, F_{ij} is the off-diagonal Kohn-Sham matrix elements between the occupied *i* (n or σ) and empty *j* (σ*) orbitals and Δε is the difference between the energy of the donor orbital (*i*) and the acceptor orbital (*j*). For the present study, we will focus on the interactions between the anti-bonding orbitals of Li^+ lone pairs and the lone pairs of F (N in the case of LiB) which are directly bonded to the cation. For LiB, LiBTB, LiBTTB and LiBTNB, the calculated results show that the order of the second-order perturbation energy is LiB (11 kcal mol^{-1}) > LiBTB (8.66 kcal mol^{-1}) > LiBTNB (8.33 kcal mol^{-1}) > LiBTTB (8.19 kcal mol^{-1}). Hence, the extent of electron transfer from the anion to the Li^+ will follow the following order: LiB > LiBTB > LiBTNB ~ LiBTTB (See Table 2). Thus, introducing NO_2 at R2 position ($BTNB^-$) and CF_3 substitution at R1 position ($BTTB^-$) of the parent structure will produce a weakly coordinated ion pair configuration. Similarly, double substitution ($BTNTB^-$) results in the generation of an ion pair with the lowest orbital interaction energy (7.86 kcal mol^{-1}), lowest dissociation energy as well as a lesser electron transfer from the anion to Li^+. Therefore, of all the anions studied in the current work, $BTNTB^-$ is the weakest anion, and LiBTNTB would be disassociated more than the other salts at the same concentration of electrolyte solutions.

3.3. Anion Oxidation Stability

Fig. 5 shows the calculated intrinsic anion oxidation potentials, E_{ox} (V vs. Li^+/Li), for the eleven anions. Previous studies showed that DFT based calculations of oxidation potential usually underestimate the experimental potential by 1-1.5 V.[31, 54, 57, 58] This is because the experimental oxidation potentials are not the real thermodynamics potential but are found by approximation based on kinetic measurements. As can be seen from the plot, except for LiB, all eleven anions are stable up to 4.5 V vs. Li^+/Li, thus can be predicted to be stable for applications in high voltage lithium-ion batteries. CH_3 substitution on R1 position of the parent structure results in a decrease in both intrinsic anion oxidation potential and dissociation constant, as compared to the parent structure (LiBTB). This is due to a weaker delocalization of the negative charge in $BTMB^-$, which renders the ion pair configuration to become more stable.

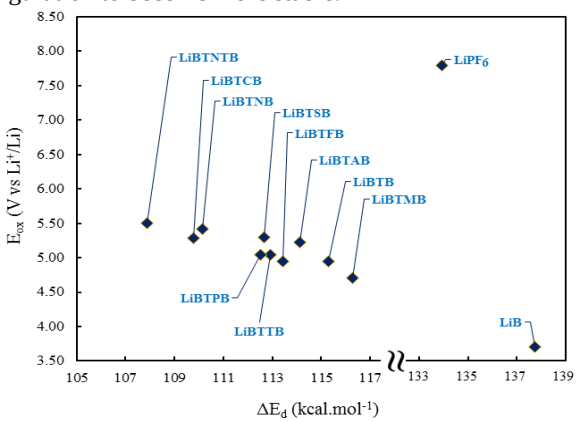

Fig. 5 Calculated intrinsic anion oxidation potentials (E_{ox} in V vs. Li^+/Li) and lithium ion pair dissociation energies in vacuum (ΔE_d in kcal mol^{-1}) calculated at B3LYP/6-311++G(d, p) level of theory.

Introducing -CF_3 at R1 position or –CN at R2 position in BTB^- will improve the intrinsic anion oxidation potentials and weakens the corresponding ion pair. However, a simple lengthening of -CF_3 to –C_2F_5, have insignificant effect on both dissociation energy and intrinsic anion oxidation potential. Scheers et al. investigated several cyano substituted fluoroalkylated benzimidazole and imidazole anions by varying the number and position of substituents and concluded that a mere increasing of the fluoroalkyl group will not significantly alter the anion oxidation stability. Similarly, based on their calculation they proposed 4,5,6,7-tetracyano-2-fluoroalkylated benzimidazolides to be a promising anion for high voltage Li-ion battery applications. However, our proposed salts exhibits much improved ΔE_d and oxidation stability compared to those reported by Scheers et al. and the commonly used PF_6^-.On another hand, introducing –NO_2 at R2 position of BTB^- will produce charge delocalized anion ($BTNB^-$) which has significantly improved the ion pair dissociation energy and the intrinsic anion oxidation potential.

The computed intrinsic anion oxidation potential and dissociation energy for the doubly substituted anion ($BTNTB^-$) was found to be better than all the anions in the current study (ΔE_d= 108 kcal mol^{-1} and E_{ox}= 5.5 V vs. Li^+/Li. Even though the calculated intrinsic anion oxidation potential of PF_6^- is higher than $BTNTB^-$, the ion pair dissociation energy of the later is much smaller. This indicates the selected salt would likely be disassociated more than $LiPF_6$ at the same concentration of electrolyte solutions. It is understood that a bigger anion will occupy a large volume and will reduce the anion diffusion in the solvent thereby decreasing the ionic conductivity. Experimental works showed that relatively bigger anions based on boron chelate complex anions with bulky aromatic substituents, such as 1,2-benzenediolato(2-)-O,O')borate (V = 255 $Å^3$ $molecule^{-1}$ and experimental E_{ox} = 3.6 V vs. Li^+/Li),[21, 59, 60] have high solubility and offer fairly conductive solutions. Hence, it can be assumed that, $BTNTB^-$ (V = 229 $Å^3$ $molecule^{-1}$) which exhibits higher intrinsic anion oxidation potential value can be a potential candidate that can be used as a lithium salt in LIBs.

4. Conclusions

We have proposed a new family of substituted heterocyclic anions based on bis(trifluoroborane)imidazolide by using density-functional calculations and identified the most promising candidates for further study as potential lithium salt for high voltage applications of lithium-ion batteries. The influence of different substituents on the most electrophilic and nucleophilic site of the parent structure were investigated with respect to ion pair dissociation energies and anion oxidative stability of the candidate molecule. The results imply that substitution at both R1 and R2 positions will produce a weakly coordinated and oxidatively stable anion.

Due to the extensive charge delocalization in the generated heterocyclic anions, the salts presented in this study will dissociate more than the widely used lithium salts for lithium ion battery. Moreover, we have also found that the ion pair dissociation energy and anion stability of $BTNTB^-$ is much improved compared to the parent structure and experimentally reported lithium salts. The calculated intrinsic anion oxidation potential for the proposed anions also indicated that the anions are stable up to 4.5 V vs. Li^+/Li, thus can be expected to be stable for applications in high voltage lithium-ion batteries. The present study shows that by introducing electron withdrawing substituents on the benzimidazole, one can design new weakly coordinating, oxidatively stable and highly dissociated anions which can offer better performance than the experimentally reported benzimidazole salts.

Acknowledgements

This work was supported by a grant from the Ministry of Economic Affairs of Taiwan, ROC (103-EC-17-A-08-S1-183). We are also grateful to the National Center of High-Performance Computing for computer time and facilities

Notes and references

Department of Chemical Engineering, National Taiwan University of Science and Technology
43 Keelung Road, Section 4, Taipei 106, Taiwan, R.O.C
E-mail: Prof.J.C.Jiang (jcjiang@mail.ntust.edu.tw), Dr. E.G. Leggesse (ermigirma@mail.ntust.edu.tw).

Electronic Supplementary Information (ESI) available: Lithium ion pair dissociation energies, ΔEd (kcal /mol) in vacuum, implicit solvation, optimized structures of the generated anions, ion-pair configurations and selected geometric parameters are provided. See DOI: 10.1039/b000000x/

1. A. N. Jansen, A. J. Kahaian, K. D. Kepler, P. A. Nelson, K. Amine, D. W. Dees, D. R. Vissers and M. M. Thackeray, *J. Power Sources*, 1999, 81-82, 902-905.
2. S. Megahed and W. Ebner, *J. Power Sources*, 1995, 54, 155-162.
3. B. Scrosati, *Electrochim. Acta*, 2000, 45, 2461-2466.
4. B. Scrosati and J. Garche, *J. Power Sources*, 2010, 195, 2419-2430.
5. V. Etacheri, R. Marom, R. Elazari, G. Salitra and D. Aurbach, *Energy Environ Sci*, 2011, 4, 3243-3262.
6. K. Nagaura and K. Tozawa, *Progress in Batteries and Solar Cells*, JEC Press Inc. and IBA Inc., Brunswick OH, USA, 1990.
7. K. Xu, *Chem. Rev.*, 2004, 104, 4303-4417.
8. A. Lex-Balducci, W. Henderson and S. Passerini, eds. X. Yuan, H. Liu and J. Zhang, CRC Press, New York, 2011, pp. 417-196.
9. G. G. Botte, R. E. White and Z. Zhang, *J. Power Sources*, 2001, 97-98, 570-575.
10. S. E. Sloop, J. K. Pugh, S. Wang, J. B. Kerr and K. Kinoshita, *Electrochem. Solid-State Lett.*, 2001, 4, A42-A44.
11. C. G. Barlow, *Electrochem. Solid-State Lett.*, 1999, 2, 362-364.
12. A. V. Plakhotnyk, L. Ernst and R. Schmutzler, *J. Fluorine Chem.*, 2005, 126, 27-31.
13. C. L. Campion, W. Li and B. L. Luch, *J. Electrochem. Soc.*, 2005, 152, A2327-A2334.
14. N. Nanbu, K. Tsuchiya, T. Shibazaki and Y. Sasaki, *Electrochem. Solid-State Lett.*, 2002, 5, A202-A205.
15. M. Handa, M. Suzuki, J. Suzuki, H. Kanematsu and Y. Sasaki, *Electrochem. Solid-State Lett.*, 1999, 2, 60-62.
16. W. Xu and C. A. Angell, *Electrochem. Solid-State Lett.*, 2001, 4, E1-E4.
17. X. Wang, E. Yasukawa and S. Kasuya, *J. Electrochem. Soc.*, 2000, 147, 2421-2426.
18. M. Schmidt, U. Heider, A. Kuehner, R. Oesten, M. Jungnitz, N. Ignat'ev and P. Sartori, *J. Power Sources*, 2001, 97–98, 557-560.
19. J. S. Gnanaraj, M. D. Levi, Y. Gofer, D. Aurbach and M. Schmidt, *J. Electrochem. Soc.*, 2003, 150 A445-A454.
20. V. Aravindan, J. Gnanaraj, S. Madhavi and H.-K. Liu, *Chemistry*, 2011, 17, 14326-14346.
21. J. Barthel, M. Wühr, R. Buestrich and H. J. Gores, *J. Electrochem. Soc.*, 1995, 142 2527-2531.
22. J. Barthel, R. Buestrich, E. Carl, H. J. Gores, E. Buestrich, E. Carl and H. J. Gores, *J. Electrochem. Soc.*, 1996, 143, 3572-3575.
23. M. Handa, S. Fukuda and Y. Sasaki, *J. Electrochem. Soc. Lett*, 1997, 144, L235-L237.

24. J. Barthel, R. Buestrich, H. J. Gores, M. Schmidt and M. Wuhr, *J. Electrochem. Soc.*, 1997, 144, 3866-3870.
25. J. Barthel, R. Buestrich, E. Carl and H. J. Gores, *J. Electrochem. Soc.*, 1996, 143, 3565-3571.
26. S. Shui Zhang, *Electrochem. Commun.*, 2006, 8, 1423-1428.
27. W. Xu, A. J. Shusterman, R. Marzke and C. A. Angell, *J. Electrochem. Soc.*, 2004, 151, A632-A638.
28. M. Armand, P. Johansson, H. Nilsson and P. Jacobsson, *Solid State Ionics*, 2003, 156, 129-139.
29. T. J. Barbarich and P. F. Driscoll, *Electrochem. Solid-State Lett.*, 2003, 6, A113-A116.
30. P. Preston, *Chem. Rev.*, 1974, 74, 279-314.
31. J. Scheers, P. Johansson, P. Szczeciński, W. Wieczorek, M. Armand and P. Jacobsson, *J. Power Sources*, 2010, 195, 6081-6087.
32. *US Pat.*, 2014.
33. G. W. T. M. J. Frisch, H. B. Schlegel, G. E. Scuseria, M. A., J. R. C. Robb, G. Scalmani, V. Barone, B. Mennucci, G. A., H. N. Petersson, M. Caricato, X. Li, H. P. Hratchian, A. F., J. B. Izmaylov, G. Zheng, J. L. Sonnenberg, M. Hada, M. Ehara, R. F. K. Toyota, J. Hasegawa, M. Ishida, T. Nakajima, Y., O. K. Honda, H. Nakai, T. Vreven, J. A. Montgomery, Jr., J. E., F. O. Peralta, M. Bearpark, J. J. Heyd, E. Brothers, K. N., V. N. S. Kudin, T. Keith, R. Kobayashi, J. Normand, K., A. R. Raghavachari, J. C. Burant, S. S. Iyengar, J. Tomasi, M., N. R. Cossi, J. M. Millam, M. Klene, J. E. Knox, J. B. Cross, V., C. A. Bakken, J. Jaramillo, R. Gomperts, R. E. Stratmann, O., A. J. A. Yazyev, R. Cammi, C. Pomelli, J. W. Ochterski, R. L., K. M. Martin, V. G. Zakrzewski, G. A. Voth, P. Salvador, J., S. D. J. Dannenberg, A. D. Daniels, O. Farkas, J. B. and J. V. O. Foresman, J. Cioslowski, and D. J. Fox, Gaussian Inc., Wallingford, CT, 2013, vol. Gaussian 09, revision D.01.
34. A. D. Becke, *J. Chem. Phys.*, 1993, 98, 5648-5652.
35. C. Lee, W. Yang and R. G. Parr, *Phys. Rev. B*, 1988, 37, 785-789.
36. P. J. Stephens, F. J. Devlin, C. F. Chabalowski and M. J. Frisch, *J. Phys. Chem*, 1994, 98, 11623-11627.
37. S. H. Vosko, L. Wilk and M. Nusair, *Can. J. Phys.*, 1980, 58, 1200-1211.
38. T. Clark, J. Chandrasekhar, G. W. Spitznagel and P. V. R. Schleyer, *J. Comput. Chem.*, 1983, 4, 294-301.
39. M. J. Frisch, J. A. Pople and J. S. Binkley, *J. Chem. Phys.*, 1984, 80, 3265-3269.
40. E. G. Leggesse and J. C. Jiang, *J. Phys. Chem. A*, 2012, 116, 11025-11033.
41. S. F. Boys and F. Bernardi, *Mol. Phys.*, 1970, 19, 553-566.
42. A. E. Reed, R. B. Weinstock and F. Weinhold, *J. Chem. Phys*, 1985, 83, 735-746.
43. A. V. Marenich, C. J. Cramer and D. G. Truhlar, *J. Phys. Chem. B*, 2009, 113, 6378-6396.
44. A. V. Marenich, J. Ho, M. L. Coote, C. J. Cramer and D. G. Truhlar, *Phys. Chem. Chem. Phys.*, 2014, 16, 15068-15106.
45. J. M. Vollmer, L. A. Curtiss, D. R. Vissers and K. Amine, *J. Electrochem. Soc.*, 2004, 151, A178-A183.
46. D. O'Hagan, *Chem. Soc. Rev.*, 2008, 37, 308-319.
47. B. E. Smart, *J. Fluorine Chem.*, 2001, 109, 3-11.
48. G. Bott, L. D. Field and S. Sternhell, *J. Am. Chem. Soc.*, 1980, 102, 5618-5626.
49. J. S. Francisco and I. H. Williams, *J. Phys. Chem*, 1990, 94, 8522-8529.
50. H. Nakai and M. Kawai, *J. Chem. Phys*, 2000, 113, 2168-2174.
51. X. Y. Li, Z. M. Xue, J. F. Zhao and C. H. Chen, *J. Power Sources*, 2013, 235, 274-279.
52. Z. M. Xue, X. F. Zhang, W. Zhou and C. H. Chen, *J. Power Sources*, 2012, 202, 336-340.
53. Z. M. Xue, J. Ding, W. Zhou and C. H. Chen, *Electrochim. Acta*, 2010, 55, 3838-3844.
54. E. Jónsson, M. Armand and P. Johansson, *Phys. Chem. Chem. Phys.*, 2012, 14, 6021-6025.
55. P. Johansson, H. Nilsson, P. Jacobsson and M. Armand, in *Phys. Chem. Chem. Phys.*, 2004, vol. 6, pp. 895-899.
56. E. Jonsson and P. Johansson, *Phys. Chem. Chem. Phys.*, 2012, 14, 10774-10779.
57. P. Johansson, *J. Phys. Chem. A*, 2006, 110, 12077-12080.
58. P. Johansson, *J. Phys. Chem. A*, 2007, 111, 1378-1379.
59. P. Johansson, *Phys. Chem. Chem. Phys.*, 2007, 9, 1493-1498.
60. W. A. Henderson, in *Electrolytes for Lithium and Lithium-Ion Batteries*, eds. T. R. Jow, K. Xu, O. Borodin and M. Ue, Springer New York, 2014, vol. 58, pp. 1-92.